This is the accepted version of this paper. The version of record is available at
https://doi.org/10.1016/j.matchemphys.2021.125034

Mechanical and thermal properties of spark plasma sintered Alumina-MWCNTs nanocomposites prepared via colloidal route

Karthikeyan Ramachandran*[1], R. Ram Subramani[2], T. Arunkumar[3] and Vignesh Boopalan[4]

[1]Department of Aerospace & Aircraft Engineering, Kingston University, London SW15 3DW, UK

[2]Department of Mechanical Engineering, Sathyabama Institute of Science & Technology, Chennai, India.

[3]Department of Mechanical Engineering, CMR Institute of Technology, Bengaluru, India

[4]Centre for CO_2 Research and Green technologies, VIT, Vellore, India.

Abstract

This paper concentrates on the fabrication of Al_2O_3-MWCNTs composites by spark plasma sintering at temperature of 1400°C by varying the percentage of MWCNTs and alumina through colloidal route. The effect of incorporating MWCNTs into Al_2O_3 were examined using physical, mechanical, and thermal properties and characterised using techniques like scanning electron microscopy, X-ray diffraction and elemental analysis. The characterized composites corresponded towards the phases of α-Al_2O_3 and carbon which were further confirmed through SEM and EDS. Densification behaviour of the nanocomposites revealed reduction in relative density with increase in MWCNTs content. Mechanical properties like Vickers hardness, fracture toughness and flexural strength of composites were analysed along with its thermal and wear behaviour under varying load and sliding distance. Composites with MWCNTs incorporation led to enhanced mechanical properties with 1 wt.% reinforced Al_2O_3 demonstrating superior hardness (17.26 ± 0.4 GPa), fracture toughness (K_{IC} = 5.6 ± 0.3 MPa.$m^{1/2}$) and flexural strength (515 ± 33 MPa) compared to the monolithic Al_2O_3.

Keywords: Alumina; MWCNTs; composites; Spark Plasma Sintering; Fracture toughness; Wear Behaviour; Thermal behaviour

---

***Corresponding Author:** Mr. Karthikeyan Ramachandran

E-mail: K1825123@kingston.ac.uk

Orcid ID: https://orcid.org/0000-0003-2246-7309

Introduction

The global demand for structural and high temperature materials has enhanced rapidly in various applications such as biomedical, aerospace and manufacturing sectors. Ceramics and composites have been successful in meeting this demand, providing industry with higher and efficient material. However, the functional and structural applications of ceramics have been limited to their brittle nature [1]. Alumina (Aluminium Oxide) is one of the extensively used ceramics owing to hardness, high temperature strength and good insulating properties. Numerous studies have been conducted by researchers to improve the mechanical properties of Alumina based composites, due to their intrinsic brittleness [2]. Paul *et al.* studied the toughening behaviour of Alumina by adding SiC whiskers into the reinforcement. The hot-pressed composites with 20 vol% SiC resulted in higher fracture toughness of 8.7 $MPa.m^{0.5}$ [3]. Whereas 3 wt.% SiC/Al_2O_3 composites fabricated through two-step microwave sintering at different temperature revealed different particle grain size and different fracture toughness which is superior to Al_2O_3 composites [4]. Similarly, Li *et al.* studied the surface hardness of zirconia-toughened alumina treated with boehmite sol which resulted in significant increase in surface hardness [5]. Various reports suggested that the reinforcement of Alumina ceramics could improve the mechanical properties of the material. However, there is evidence reduction in desirable properties such as hardness and young's modulus [6].

Along with different mechanical properties, thermal and tribological properties such as wear, thermal conductivity also plays a crucial role in determining the service life of the component in structural applications. The need for wear and thermal properties in structural applications have been studied by various researchers for different materials including metals, alloys and various ceramics and its composites for many years [7, 8]. The use of ceramics such as SiC and Al_2O_3 are limited in structural applications due to the necessity of high friction tolerance which are affected by brittleness of the ceramics. Researchers have tried to reduce the friction by introducing lubrication, reinforcement, and coating systems however, the wear on the ceramics still represents a significant challenge [9]. However, the micro-sized materials have provided with various contradictions which have made various researchers move towards new approach of reinforcing nanomaterials such as carbon nanotubes and graphene into the ceramic system [10, 11, 12]. Carbon nanotubes have been a keen research due to its remarkable mechanical and thermal properties which make them appropriate reinforcement of nanocomposites [13]. Siegel *et al.* reported that addition of 10 vol.% CNT into alumina composites increased the fracture toughness up to 24 % compared to monolithic alumina [14]. The use of CNT based ceramic composites are not only limited to structural applications whereas some studies have been conducted to determine its usage in thermal and environmental barrier applications [15]. Previous reports on reinforcing multi-walled carbon nanotubes (MWCNTs)

with SiC and YSZ ceramics for thermal barrier coatings and structural applications have resulted in increased mechanical and thermal properties of the ceramic composites [16, 17]. In some cases, the reinforcement of CNTs with alumina failed in showing any improvement in mechanical properties [18].Puchy *et al.* reported the wear resistance of alumina at higher concentration of CNT (>5%) shown reduction in frictional coefficient [19]. According to the reference [20], a decrease in the mechanical properties have been reported when the CNT content increases over 10%. Researchers have tried out different material processing and fabrication techniques to compensate the mechanical and thermal properties of the CNTs reinforced ceramics [21, 22, 23, 24]. However, certain fabrication techniques did not yield the desirable densification of the CNT reinforced composites [25]. However, our previous studies on the usage of spark plasma sintering based fabrication techniques yielded high relative density with uniform distribution of CNTs [16, 17].

This shows a constant gap in understanding the mechanical, thermal and wear properties of the MWCNTs reinforced Al_2O_3 due to various contradictions on the results reported by various researchers. These contradictions could be due to the fabrication techniques, powder processing associated with the ceramic composites. Therefore, this study focuses on analysing the mechanical behaviour, thermal and wear behaviour of Al_2O_3/MWCNTs nanocomposites fabricated via spark plasma sintering technique using colloidal route to understand the precise quantity of MWCNTs required for improving the properties of the composites for its usage in structural and barrier coating applications.

Materials and Methods

Powder Preparation & Fabrication

Table 1. Different composition of the fabricated composites

Samples	MWCNTs (wt.%)	Al_2O_3 (wt.%)
AC0	0	100
AC1	1	99
AC3	3	97
AC5	5	95

Powder preparation for the Alumina-MWCNTs nanocomposites comprised of commercially available Al_2O_3 nano-powders procured from MK Industries, Canada with average particle size of 20-30nm and purity over 99% and MWCNTs with purity >97% and outer diameter ranging between 20-30nm which were synthesised through thermal catalytic chemical co-impregnation technique (TC-

CVD) with Fe/MgO as catalysts [26]. The composite nano-powders were synthesised though colloidal route with help of three different physical dispersion techniques such as ultrasonication, ball milling and rotary evaporator as illustrated in Figure 1. The MWCNTs were dispersed into an ethanol and water medium in a ratio of 3:2 with 0.5 wt.% sodium hexametaphosphate as dispenser agent and ultrasonicated (probe-ultrasonicator, Oscar PR600MP) at high frequency of 50 KHz for 20 minutes. After sonication using high frequency acoustic waves, nano-powders of alumina are introduced into the solution and vigorously stirred using magnetic stirrer to enhance the blending between alumina and MWCNTs. The obtained slurry was ball milled at constant speed of 300 rpm for 5 hours and further dried using rotary evaporator at temperature of 100°C for 12 hours [16, 17]. The synthesized nano-powders with different MWCNTs percentages as represented in Table 1 were fabricated using spark plasma sintering at constant temperature of 1400°C with dwelling time of 10 minutes. The heating rate of 300°C/min was applied from room temperature to 600°C with a dwell time of 2 minutes further a heating rate 100°C/min was maintained for the remaining 8 minutes. The cooling rate of the composites were kept constant at 70°C/min to avoid cracks.

Characterisation and Methods

The fabricated nanocomposites were studied for its phase composition using X-ray diffractometer (smart lab-RIGAKU, Japan) with varying 2θ values between 0° to 90° and current of 100mA, wavelength of 1.54056Å with step of $0.05°s^{-1}$ and operational target voltage of 30KV. Scanning electron microscopy (SEM) and elemental analysis was carried out at different spots of the composites to ensure homogenous distribution of the MWCNTs throughout the samples by coating the samples with Pt/Gd using sputter coatings.

The composites were studied its theoretical density through rules of mixtures and bulk density through Archimedes method with help of water as immersion medium. Relative density was also calculated and further detailed discussion on densification behaviour is provided in following section. Vickers hardness (ASTM C1327) were evaluated with help of diamond indenter at load of 10N and dwell time of 20 seconds. Diagonal lengths of the composites were measured using SEM and indentation fracture toughness was evaluated according to previous study using Evans and Charles equation [16, 17]. Flexural strength of the composites were measured at room temperature -point bending tests with inner span of 20 mm and outer span of 40 mm using samples dimensions 3 mm × 4 mm × 45 mm. Pin-on-disk method (DUCOM TR-20LE-PHM-400- ASTM G99) was utilised to study the wear resistance of the composites under room temperature condition with varying load (10 & 20N), time (30 & 60 minutes) and sliding distance (100 & 400m) at constant sliding speed of 0.523m/s. Thermal conductivity and diffusivity of the samples was measured using Netzsch DIL

LFA-467 dilatometer with sample size of 10×10×4 mm under argon temperature (vacuum environment).

Results and Discussion

Microstructure, Phase & Elemental Analysis

The X-ray diffraction patterns of the composites along with Al_2O_3 and synthesized MWCNTs are represented in Fig. 2. The XRD pattern of MWCNTs were adopted from previous work on synthesis of MWCNTs through TCCVD method [26]. The major peaks of MWCNTs corresponded at 26°, 43° and 57° whereas in Al_2O_3 the major peaks were at 25°, 35°, 37°, 44°, 55° and 68°. The high intensity peaks of Alumina and MWCNTs matched the corresponding patterns of the material (MWCNTs-JCPDS file no. 26-1079 and alumina JCPDS file no. 42-1468) available at JCPDS software (Rigaku Cooperation) and crystalline size of the MWCNTs and alumina was calculated using Scherrer equation [26]. MWCNTs had a crystalline size of 1.04 nm with lattice strain of 0.6661 which was reported in our previous work [26] and alumina had 46 nm with lattice stain of 3.6×10^{-3}. The peaks of the Alumina in the XRD corresponded towards the α-alumina even after sintering showing the high stability of the alumina powder at high temperature. In the composites AC1-AC5, the major peaks corresponded to alumina. However, small intensities of CNT peaks were also found on the composites at 2θ values 26°, 32°, 44° and 77° of proving the homogenous distribution of MWCNTs through ultra-sonification and ball milling prior to sintering. Even through the intensity of the peaks corresponding to CNTs were less, a further elemental analysis was carried out to determine the presence of carbon content on the composites. The elemental analysis of the composites is plotted in the Fig. 3 where the presence of Al and Oxygen were thoroughly visible along with carbon and impurities such as Pt, Gd which were utilised for coating. Through elemental analysis, the presence and composition of carbon was found to be a bit higher than the actual percentile values added into the compositions. This may be due to the fabrication process taken place in the graphite die which could have increased the composition of carbon.

The SEM images of aluminium oxide and its nanocomposites are shown in Fig. 4(a & d). The SE images are obtained in closer microscopic scale of 10 μm to 20 μm to understand the morphological structure of the samples. The morphology of the samples was dependent on the MWCNT content. The Fig. 4(a) illustrates the microstructure of alumina ceramic which has coarse grain sizing with loosely packed alumina materials. However, incorporation of 1 wt.% MWCNTs in AC1 led to grain refinement with reduced flutes on the surfaces of the sample (Fig. 4(b)) which could be a result of increased interfacing bonding between CNTs and alumina in the composites. However, on the other hand incorporation of 3 % MWCNTs in AC3 composites shown a very fine grain refinement with no

pores on the surfaces due to higher interfacing bonding and Van der Waals forces of attraction of MWCNTs as shown in Fig. 4(c) [17]. But with the drawback of increased MWCNTs addition, the AC5 composite again shown a semi-fine morphological surface compared to AC3, this could be due to the higher concentration of MWCNTs led to agglomeration which resulted in reduced Van der Waals forces of attraction between the MWCNTs and alumina. Further, the agglomeration of MWCNTs also reduce the joule heating effect on the composites while sintering using spark plasma sintering [16]. The effect of reduced joule heating could affect the microstructure, relative density of the composites. Further, in Fig. 4(d) the surface consisted of open and closed pores which could be the reason for reduction in relative density. The presence of open and closed pores could be a result of sintering temperature as the transition of open pores to closed pores could occur at a temperature of 1050°C in alumina composites [27]. Line interpolation technique was utilised to study the grain size of the composites though SEM images and revealed that the Alumina without any MWCNTs incorporation shown average grain size of ~35nm after sintering. However, MWCNTs reinforced ceramics composites shown finer grain size of ~20-30nm in AC5.

Densification Behaviour

The Fig. 5 illustrates the theoretical, bulk relative densities of the sintered nanocomposites. The densification behaviour of the composites varies under the similar SPS condition from 98 % for AC0 to 97.2 % for AC1, 95.8 % for AC3 to 93.4 AC5, respectively. Likewise, there is slight variation in the theoretically calculated density and bulk densities. This variation in the results from the theoretical and bulk density could have been due to the sintering effect of the composites which could have affected the density of the constituents. Even so, variation in the density is negligible (~0.15 g/cm^3) which can be neglected in certain cases. From Figure 1, it is evident that the density dropped to lower values with an increase in weight percentage of MWCNTs content in the composites. This may have been due to composition of MWCNTs lead to pinning down the grain boundaries of the composites resulting in inhabitation of grain growth which restrict densification [28]. Furthermore, higher concentrations of MWCNTs in the composite could lead to agglomeration that increases the open pores network leading to additional reduction in density [29]. The higher concentration of MWCNTs in AC3 and AC5 could have been the reason for the decrease in density of the composites. The agglomeration of MWCNTs present inside the composites forms a continuous layer which decrease the Joules heating by providing low resistance under sintering conditions [30].

Hardness & Fracture Toughness

The Fig. 6 plots the Vickers hardness and fracture toughness of the nanocomposites evaluated by measuring the diagonal lengths of the intender measured from SE images. The variation in the Vickers hardness was uniform with highest values of hardness was noted for AC1 (17.26 ± 0.4 GPa) and AC3

(17.11 ± 0.3 GPa). These values were comparatively higher than the AC0 (15.72 ± 0.3 GPa) due to the incorporation of MWCNTs which were uniformly distributed onto the matrix through the ultrasonication techniques and spark plasma sintering process which increased the Van der Waals forces of attraction between the CNTs and alumina. Hah *et al.* reported that the increase in hardness could have been a result of change in morphology and grain size which could have been possible even in this case as the variation in morphology was visible in Fig. 4 under SE image [31]. On the other side, hardness of the AC5 (14.21 ± 0.4 GPa) reduced by ~20% and ~18.5% compared to AC1 and AC3. The reduce in the harness in AC5 could be due to the agglomeration of CNTs with nanopores which deteriorate the hardness by weaking the interfacing bonding between alumina and MWCNTs. These hardness results thus obtained through the experimental method demonstrates that the hardness property depends on the MWCNTs reinforcement. Nevertheless, the values reported in this report are higher compared to the previous literature reports owing to the homogenous distribution of MWCNTs which surfaced due to pro-longed high acoustics ultrasonication process and ball milling prior to fabrication [32].

The fracture toughness (K_{IC}) of the nanocomposites were calculated using the indentation method by precisely measuring the diagonal length and crack lengths of the Vickers hardness intender acted on the composites using SEM. The fracture toughness of alumina and its composites increased with incorporation of MWCNTs with AC0 showing 3.98 ± 0.4 MPa.m$^{1/2}$ which further enhanced upto ~33% and ~40% for AC1 (5.6 ± 0.3 MPa.m$^{1/2}$) and AC3 (5.92 ± 0.3 MPa.m$^{1/2}$). The AC3 acted as a threshold limit for the increase in the fracture toughness, as the toughness dropped by ~8% for AC5 sample (5.42 ± 0.2 MPa.m$^{1/2}$) with 2% increase in MWCNTs percentage compared to AC3. However, the AC5 maintained higher fracture toughness than the AC0 or the monolithic alumina ceramic. This trend was reported by various authors along with our previous reports on SiC and YSZ reinforced with varying MWCNTs percentage reported the same [16, 17].

In case of MWCNTs, reinforced ceramic composites (AC1, AC3 & AC5), the colloidal technique undertaken prior to fabrication played a crucial role in improvement of fracture toughness values. The ultrasonication of MWCNTs in ethanol solution using high frequency acoustic waves of 50KHz for 20 minutes led to full dispersion of CNTs into the ethanol solution. Furthermore, magnetic stirring, ball milling and rotary evaporation aided homogenous distribution of MWCNTs on the ceramic particles. However, the K_{IC} of the AC5 was reduced compared to AC1 and AC3 due to the presence of pores and weaker interfacial bonding between the MWCNTs and alumina. Various works have reported the toughening mechanism such as crack deflection, fiber pull-out and crack bridging associated with the fiber reinforced composites. In the case of MWCNTs reinforced alumina composites, the SE image illustrated in Fig. 7(b) shows the fiber bridging and pull-out mechanism acting as key toughening mechanism for enhancing fracture toughness in AC1 and AC3 composites.

When a fracture load was applied onto the surface of composite, the spiral MWCNTs structure untangles and expands leading to the spring behaviour which increases the fracture toughness [17]. However, in case of AC5 the amount of MWCNTs present on the surface restrict the untangling of MWCNTs which reduce the fracture toughness along with the reduced pinning effect of CNTs which reduce the bonding between CNTs and ceramics.

Flexural Strength

The bending strength/flexural strength of the alumina and its composites are reported in Fig. 8 where a constant decrease was observed in the bending strength with increase in MWNCTs content with threshold of 1% MWCNTs. The monolithic alumina ceramic displayed bending strength of 423 ± 40 MPa whereas the composite with 1wt% MWCNTs showing a drastic increase in the flexural strength of 515 ± 33 MPa which is an enhancement of ~20% than the reference alumina. This drastic increase of the flexural strength on the AC1 could be due to the higher young's modulus of CNTs (~1 TPa) and higher relative density of AC1. The higher flexural modulus of the CNTs with uniform distribution though the ultrasonication process led to the increased density of AC0 and AC1 samples. The homogenous distribution of MWCNTs throughout the alumina matrix in AC1 enhanced the pinning effect of MWCNTs with the grain boundaries leading to increase in flexural strength. However, pinning effect was reduced with higher concentration of MWCNTs as the samples (AC3 and AC5) with 3 wt.% and 5 wt.% MWCNTs content had flexural strength of 378 ± 30 MPa and 283 ± 35 MPa compared the Al_2O_3. Similar trend in the flexural strength was observed and reported in literatures where the flexural strength dropped from 2.5 vol.% [25, 33]. The deterioration of the flexural strength in the AC3 and AC5 composites with increase in MWCNTs content could be due to the drastic drop in the relative density caused by excessive MWCNTs agglomeration which resulted in reduction of sintering effect creating pores throughout the surfaces. Additionally, the decrease in the elastic modulus of CNT-Alumina composites could be also based on the short fiber reinforced composites theory and rules of mixtures theory where the reinforcing efficiency of short fibers are lower than the longer fibers [25].

Some researchers have disputed the reports obtained though indentation fracture techniques as the method involves indirect medium by measuring fracture measurements through cracks propagating from the Vickers hardness testing [17, 34]. So, another approach of SEVNB (single edge V-notch beam) was utilised with help of flexural strength samples to understand the fracture toughness. Through SEVNB method, the fracture toughness depended on MWCNTs content as that of indentation fracture toughness. The AC0 samples demonstrated fracture toughness of 3.5 ± 0.4 $MPa.m^{1/2}$ which further enhanced to 5.2 ± 0.6 $MPa.m^{1/2}$ for AC1 and 6.18 ± 0.3 $MPa.m^{1/2}$ for AC3 samples which is ~48 % and ~76 % compared to monolithic alumina. This increase could be related

to the mechanisms such as CNT bridging, crack branching and deflection mechanisms [16, 17]. However, in AC5 the fracture toughness reduced to 4.9 ± 0.3 MPa.m$^{1/2}$ as verified in the other fracture toughness method. The agglomeration of high CNTs quantity in AC5 reduced the interfacing bonding which decreased the fracture toughness of the samples. The Fig. 9 illustrates the comparison of SEVNB and indentation fracture toughness mechanisms. Comparing the indentation and SEVNB methods, the mechanisms of MWCNTs reinforced alumina were same as bridging and pull-out as key factors. However, there was variation in the fracture toughness values as SEVNB shown ~12% reduction in AC0 and ~7% in AC1 composites.

Wear Behaviour

The specific wear rates (SWR) of the alumina & its nanocomposites was experimentally evaluated using pin-on disc method by varying the parameters such as load, time and sliding distance as shown in Table 2 according to ASTM standards. The SWR of the monolithic alumina and its nanocomposites shows that the wear rate of the composites was highly dependent of all the parameters (sliding distance, time and load) and MWCNTs content of the composites. The results attained from wear study are plotted in the Fig. 10(a & b) with respect to the MWCNTs content and time.

Table 2. Parameters utilised for pin-on disc wear test

Parameters	Values
Load	10 and 20 N
Time	30 and 60 minutes
Sliding Distance	100 & 400 m

The Fig. 10(a) illustrates the SWR of the alumina and its composites for sliding distance of 100 m with varying load and time. Monolithic alumina under the load of 10 N and sliding time of 30 and 60 minutes expressed higher SWR compared to 1 wt.% MWCNTs reinforced alumina (AC1). However, the incorporation of MWCNTs above 1wt.% led to increase in the wear rate of the composites with AC5 demonstrating ~11% increase than the AC0 composites. The incorporation of the MWCNTs upto the 3wt.% acted as threshold limit with 1% MWCNTs demonstrated higher wear resistance and any further addition resulted in decreased wear resistance. The incorporation of MWCNTs into the alumina matrix led to decrease in SWR such as AC1 shown a reduction of ~13% compared to AC0 composites. This decrease in the specific wear rate of the AC1 composites could be due to the homogenous distribution of MWCNTs which enhanced the interfacing bonding between alumina and CNTs which reduced lower wear material loss. Further, lubrication property of MWCNTs could also increase the wear resistance in AC1 and AC3. But in AC5 composites, the higher concentration of MWCNTs led to agglomeration which reduced the relative density leading to reduced bonding which resulted in decrease wear resistance. With increase in wear load, the SWR of the composites exhibited

double the wear rate compared to lower load with AC1. These results were contradictory to the report by J.W. An *et al.* as friction coefficient of the composites decreased with increasing MWCNT content with a ceiling of 12.5 vol.% [20]. However, the increase in frictional coefficient was reported by Hanzel *et al.* which is supportive to the current study where the frictional coefficient determined to attain minimum and maximum values at certain wear experiments [35].

On the other hand, with increase in sliding distance, SWR increased for same loading conditions with ~33% increase in SWR of AC0 (4.98×10^{-7} mm^3/Nm) compared to AC0 (3.56×10^{-7} mm^3/Nm) in lower sliding distance (100 m). Likewise, nanocomposites AC1, AC3 and AC5 exhibited almost constant increase of ~30% compared to the lower sliding distance. The Fig. 11(a, b & c) shows the topography of the wear tracks which consisted of non-continuous debriefs with dark and light spots on the surfaces. The dark spots had lesser effect of the wear whereas the light spots shown continuous damage on the surfaces of the wear with large crack propagation along the path of the wear track. The light spots on the surfaces resulted in the higher frictional coefficient whereas the darker spots on the surfaces shown reduced wear tracks and debriefs. Comparing wear topographic images the cracks formed on the surfaces of AC1 were lesser than the AC0 composites. This may be due to higher interfacing bonding and lubricating property of MWCNTs reinforced with alumina.

Thermal Properties

Alumina and its nanocomposites were studied for thermal conductivity and expansion at room temperature (plotted in Figure 9). The trend of thermal conductivity at room temperature of alumina ceramic and its composites reinforced by MWCNTs shows a decrease with increasing MWCNT content. Alumina ceramic displayed highest thermal conductivity of 37 W/mK compared to its counterparts AC1 (31 W/mK), AC3 (20.74 W/mK) and AC5 (13.26 W/mK) composites sintered through same SPS technique under same condition. This reduction in the thermal conductivity could be due to incorporation of MWCNTs which enhance the interface thermal resistance between the ceramic and CNTs which resist the heat transport through the matrix. Also, the springy or twists formed in the MWCNTs while sintering process blocks off the traveling phonons leading to reduced thermal conductivity. Moreover, due to the Van der Waals forces of attraction between the CNTs, the CNT powders incorporated into ceramic matrix agglomerate forming bundles and ropes shaped nano-structured (Fig. 7(b)) which supress the phonon-phonon scattering. This trend was reported by Hazel *et al.* where the team stated a reduce in the conductivity due to the incorporation of MWCNTs into the ceramic matrix [35]. However, Kumari *et al.* reported an enhancement in the thermal conductivity due to the uniform distribution of MWCNTs by growing CNTs onto alumina matrix [36]. However, in this study, the SPS fabrication process led to close packing of MWCNTS with alumina powder resulting in enhanced grain sizing which reduced the pores. These closed and open

pores were responsible for releasing the thermal stress acting on the sample leading to the reduced conductivity.

The thermal diffusivity of the monolithic Al_2O_3 and its composites reinforced with MWCNTs were studied using dilatometer under room temperature and plotted in Fig. 9. The diffusivity of the Al_2O_3 ceramic was evaluated to be 7.52 mm^2/s which enhanced by ~18% for AC1 sample (9.23 ± 0.3 mm^2/s). This increase in thermal diffusivity could be a result of homogenous distribution of CNTs which transfer the heat throughout the surfaces. On the other hand, AC3 and AC5 shown reduction in the thermal diffusivity values by ~32% and ~35% related to AC1 samples. The values of the AC3 and AC5 sampled dropped less than the monolithic ceramic reference due to the higher aspect ratio of MWCNTs increased the agglomeration on the surfaces of the composites. These agglomerated CNTs can led to scattering of heat act on the samples leading to the reduction of thermal diffusivity which was in argument with Moohjimoh *et al.* and Kumari *et al.* [36, 37].

Conclusion

Alumina/MWCNTs nanocomposites with varying MWCNTs (1, 3 &5 wt.%) were processed through colloidal route and sintered with help of spark plasma sintering at 1400°C. Highly dense nanocomposites with uniform and homogenous MWCNTs distribution with negligible amount of open and closed pores were fabricated. The microstructural and phase characterization revealed the high purity of composites with homogenous distribution of CNTs onto the alumina matrix. The mechanical, thermal and wear properties of the composites improved significantly compared to the monolithic alumina fabricated via same technique. The composite with 1 wt.% MWCNTs (AC1) shown significantly promising mechanical properties such as Vickers hardness (17.26 ± 0.4 GPa), fracture toughness (5.6 ± 0.3 $MPa.m^{1/2}$) and flexural strength (515 ± 33 MPa) which were higher than the other composites and Al_2O_3. This increase in the fracture toughness and Vickers hardness could have been crack deflection and bridging behaviour of MWCNTs. The specific wear rate of AC1 were comparatively lower than others showing its higher wear resistance and reduction in thermal conductivity in room temperature was result of incorporation of MWCNTs which led to supressing phonon travels in the samples.

Acknowledgement

Authors would also like to thank Dr. Joseph C. Bear of Kingston University, Chemistry department for his feedbacks and suggestions on the work.

Declaration of competing interests

The authors declare that they have no known competing financial interest or personal relationship that could have appeared to influence the work reported in this paper.

References

[1] G.-D. Zhan and A. K.Mukherjee, "Carbon Nanotube Reinforced Alumina-Based Ceramics with Novel Mechanical, Electrical, and Thermal Properties," *International Journal of applied ceramic Technology,* vol. 1, no. 2, pp. 161-171, 2005.

[2] I. Momohjimoh, M. Hussein and N. A. Aqeeli, "Recent Advances in the Processing and Properties of Alumina–CNT/SiC Nanocomposites," *Nanomaterials ,* vol. 9, no. 1, p. 86, 2019.

[3] P. Bercher and G. Wei, "Toughening behavior in SiC-whisker-reinforced Alumina," *Journal of the American Ceramic Society,* vol. 67, no. 12, pp. C267-269, 1984.

[4] D. Hong, Z. Yin, S. Yan and W. Xu, "Fine grained Al2O3/SiC composite ceramic tool material prepared by two-step microwave sintering," *Ceraic International,* vol. 45, no. 9, pp. 11826-11832, 2019.

[5] Y. Li, H.-E. Kim and Y.-H. Koh, "Improving the surface hardness of zirconia toughened alumina (ZTA) composites by surface treatment with a boehmite sol," *Ceramic International,* vol. 38, no. 4, pp. 2889-2892, 2012.

[6] D. Tang, H.-B. Lim, K.-J. Lee, C.-H. Lee and W.-S. Cho, "Evaluation of mechanical reliability of zirconia-toughened alumina composites for dental implants," *Ceramics International,* vol. 38, no. 3, pp. 2429-2436, 2012.

[7] M. Zandrahimi, M. Bateni, A. Poladi and J. Szpunar, "The formation of martensite during wear of AISI 304 stainless steel," *Wear,* vol. 263, no. 1-6, pp. 674-678, 2007.

[8] R. Barkallah, R. Tattak, N. Guermazi, K. Elleuch and J. Bouaziz, "Mechanical properties and wear behaviour of alumina/tricalcium phosphate/titania ceramics as coating for orthopedic implant," *Engineering Fracture Mechanics,* vol. 241, no. 107399, 2021.

[9] N. Sharma, S. Alam, B. Roy, S. Yadav and K. Biswas, "Wear behavior of silica and alumina-based nanocomposites reinforced with multi walled carbon nanotubes and graphene nanoplatelets," *Wear,* Vols. 418-419, pp. 290-304, 2019.

[10] B. F. Achachlouei and Y. Zahedi, "Fabrication and characterization of CMC-based nanocomposites reinforced with sodium montmorillonite and TiO2 nanomaterials," *Carbohydrate polymers ,* vol. 199, pp. 415-425, 2018.

[11] T. Arunkumar, V. Pavanan, V. Murugesan, V. Mohanavel and K. Ramachandran, "Influence of Nanoparticles Reinforcements on Aluminium 6061 Alloys Fabricated via Novel Ultrasonic Aided Rheo-Squeeze Casting Method," *Metals and Materials International,* 2021.

[12] R. J. Colchester, C. A. Mosse, D. S. Bhachu, J. C. Bear, C. J. Carmalt, I. P. Parkin, B. E. Treeby and a. A. E. D. Ioannis Papakonstantinou, "Laser-generated ultrasound with optical

fibres using functionalised carbon nanotube composite coatings," *Applied Physics Letters ,* vol. 104, no. 173502, 2014.

[13] G. G. Wildgoose, E. J. Lawrence, J. C.Bear and P. D. McNaughter, "Enabling electrochemical studies of chemically-modified carbon nanotubes in non-aqueous electrolytes using superparamagnetic nanoparticle-nanotube composites co-modified by diazirine molecular “tethers”," *Electrochemistry Communications ,* vol. 13, no. 10, pp. 1139-1142, 2011.

[14] R. Siegel, S. Chang, B. Ash, J. Stone, P. Ajayan, R. Doremus and L. Schadler, "Mechanical behavior of polymer and ceramic matrix nanocomposites," *Scripta Materialia,* vol. 44, no. 8-9, pp. 2061-2064, 2001.

[15] K. Goyal, H. Singh and R. Bhatia, "Behaviour of carbon nanotubes-Cr2O3 thermal barrier coatings in actual boiler," *Surface Engineering ,* vol. 36, no. 2, pp. 124-134, 2020.

[16] T.Arunkumar, R.Karthikeyan, R. Subramani, M.Anish, J.Theerthagiri, R. Boddula and J.Madhavan, "Effect of MWCNTs on Improvement of Fracture Toughness of Spark Plasma Sintered SiC Nano-Composites," *Current Analytical Chemistry,* vol. 16, no. 1, 2020.

[17] T.Arunkumar, G.Anand, R. Subbiah, R.Karthikeyan and J. Jeevahan, "Effect of multiwalled carbon nanotubes on improvement of fracture toughness of spark-plasma-sintered Yttria-stabilized Zirconia nanocomposites," *Journal of Materials Engineering and Performance,* Feb 2021.

[18] C. Laurent, A. Peigney, O. Dumortier and A. Rousset, "Carbon nanotubes–Fe–Alumina nanocomposites. Part II: microstructure and mechanical properties of the hot-Pressed composites," *Journal of the European Ceramic Society,* vol. 18, no. 14, pp. 2005-2013, 1998.

[19] V.Puchy, P.Hvizdos, J.Dusza, F.Kovac, F.Inam and M.J.Reece, "Wear resistance of Al2O3–CNT ceramic nanocomposites at room and high temperatures," *Ceramic International ,* vol. 39, no. 5, pp. 5821-5826, 2013.

[20] J.-W.An, D.-H.You and D.-S.Lim, "Tribological properties of hot-pressed alumina–CNT composites," *Wear,* vol. 255, no. 1-6, pp. 677-681, 2003.

[21] R. Ma, J. Wu, B. Wei, J. Liang and D. Wu, "Processing and properties of carbon nanotubes–nano-SiC ceramic," *Jorunal of Materials Science ,* vol. 33, pp. 5243-5246, 1998.

[22] L. Zhu, C. Tian, J. Zhai and R. Yang, "Sol–gel derived carbon nanotubes ceramic composite electrodes for electrochemical sensing," *Sensors and Actuators B : Chemical ,* vol. 125, no. 1, pp. 254-261, 2007.

[23] O. Popov, J. Vleugels, E. Zeynalov and V. Vishyakov, "Reactive hot pressing route for dense ZrB2-SiC and ZrB2-SiC-CNT ultra-high temperature ceramics," *Journal of the European Ceramic Society ,* vol. 40, no. 15, pp. 5012-5019, 2020.

[24] K. Goyal, H. Singh and R. Bhatia, "Experimental investigations of carbon nanotubes reinforcement on properties of ceramic-based composite coating," *Jorunal of the Australian Ceramic Society ,* vol. 55, pp. 315-322, 2019.

[25] S. Zhang, W. Fahrenholtz, G. Hilmas and E. Yadlowsky, "Pressureless sintering of carbon nanotube–Al2O3 composites," *Journal of the European Ceramic Society,* vol. 30, no. 6, pp. 1373-1380, 2010.

[26] T.Arunkumar, R.Karthikeyan, R. Subramani, K.Vishwanathan and M.Anish, "synthesis and characterisation of multi-walled carbon nanotubes (MWCNTs), International Journal of Ambient Energy," *International Journal of Ambient Energy,* vol. 41, no. 4, pp. 452-456, 2020.

[27] N. Djourelov, Y. Aman, D. Sillou and P. Nedelec, "Pore closure in spark plasma sintered alumina studied by variable energy positrons," *The European Physical Journal Applied Physics,* vol. 57, no. 2, p. 20402, 2012.

[28] S.-L. Shi and J. Liang, "Effect of Multiwall Carbon Nanotubes on Electrical and Dielectric Properties of Yttria-Stabilized Zirconia Ceramic," *Journal of the American Ceramci Soceity,* vol. 89, no. 11, pp. 3533-3535, 2006.

[29] R. Hassan, A. Nisar, S.Ariharan, F. Alam, A. Kumar and K. Balani, "Multi-functionality of carbon nanotubes reinforced 3 mol% yttria stabilized zirconia structural biocomposites," *Materials Science and Engineering: A,* vol. 704, pp. 329-343, 2017.

[30] A.Nisar, S.Ariharan, T.Venkateswaran, N.Sreenivas and K.Balani, "Oxidation studies on TaC based ultra-high temperature ceramic composites under plasma arc jet exposure," *Corrosion Sciences ,* vol. 109, pp. 50-61, 2016.

[31] S.R.Hah, T.E.Fischer, P.Gruffel and C.Carry, "Effect of grain boundary dopants and mean grain size on tribomechanical behavior of highly purified α-alumina in the mild wear regime," *Wear,* vol. 181/183, pp. 165-177, 1995.

[32] T. Zhang, L. Kumari, G. Du, W. Li, Q. Wng, K. Balani and A. Agarwal, "Mechanical properties of carbon nanotube–alumina nanocomposites synthesized by chemical vapor deposition and spark plasma sintering," *Composites Part A: Applied Science and Manufacturing ,* vol. 40, no. 1, pp. 86-83, 2009.

[33] O. Hanzel, F. Lofaj, J. Sedlacek, M. Kabatova, M. Tatarkova and P. Sajgalik, "Mechanical and tribological properties of alumina-MWCNTs composites sintered by rapid hot-pressing," *Journal of the European Ceramic Society ,* vol. 37, no. 15, pp. 4821-4831, 2017.

[34] X. Wang, N. Padture and H. Tanaka, "Contact-damage-resistant ceramic/single-wall carbon nanotubes and ceramic/graphite composites," *Nature Materials ,* vol. 3, pp. 539-544, 2004.

[35] O. Hanzel, J. Sedlacek, E. Hadzimova and P. Sajgalik, "Thermal properties of alumina–MWCNTs composites," *Journal of the European Ceramic Society ,* vol. 35, no. 5, pp. 1559-1567, 2015.

[36] L. Kumari, T. Zhang, G. Du, W. Li, Q. Wang, A. Datye and K. Wu, "Thermal properties of CNT-Alumina nanocomposites," *Composites Science and Technology,* vol. 68, no. 9, pp. 2178-2183, 2008.

[37] I. Momohjimoh, S. Nouari, M. Hussein, T. Laoui and N. Al-Aqeeli, "Thermal behaviour of spark plasma sintered Alumina-based nanocomposites," *Arabian Journal for Science and Engineering ,* vol. 44, pp. 6013-6028, 2019.

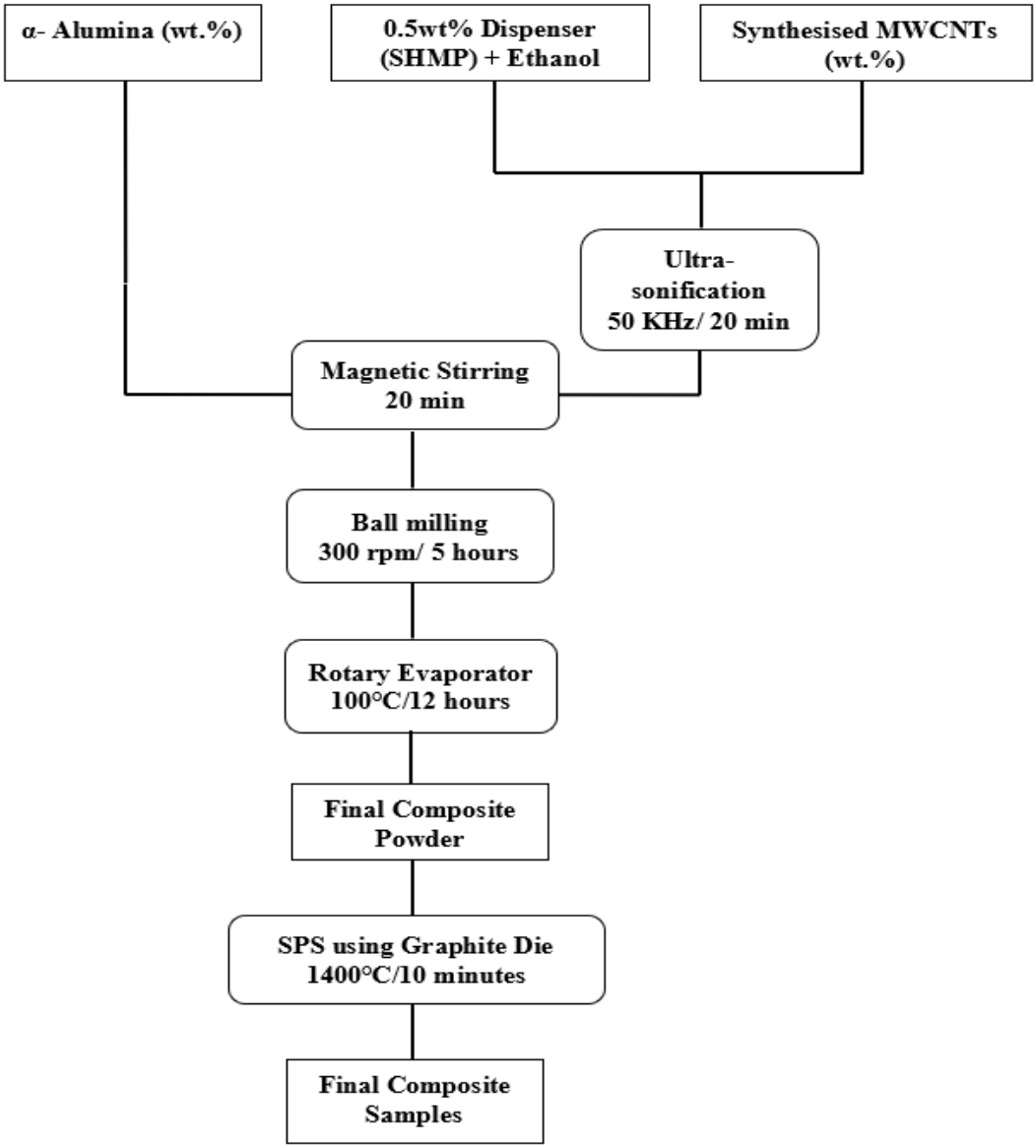

Figure 1. Schematics of powder processing and spark plasma sintering process for Alumina/MWCNTs composites.

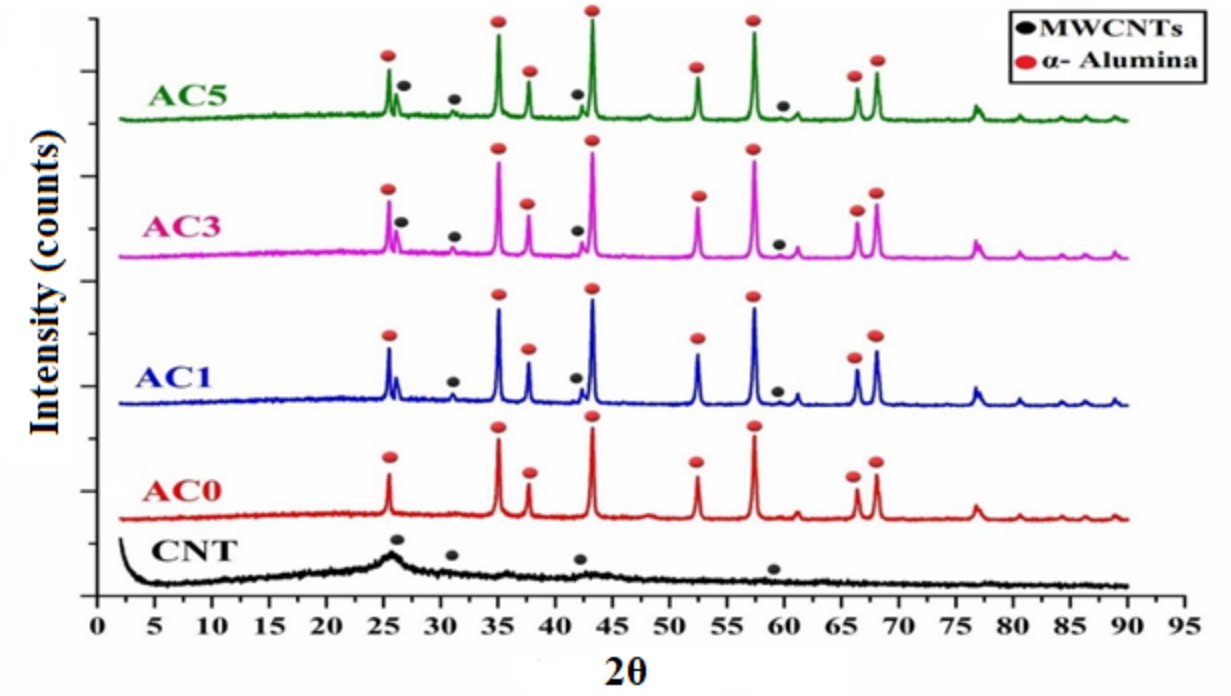

Figure 2. X-ray diffraction patterns of synthesised MWCNTs and spark plasma sintered Alumina and its composites.

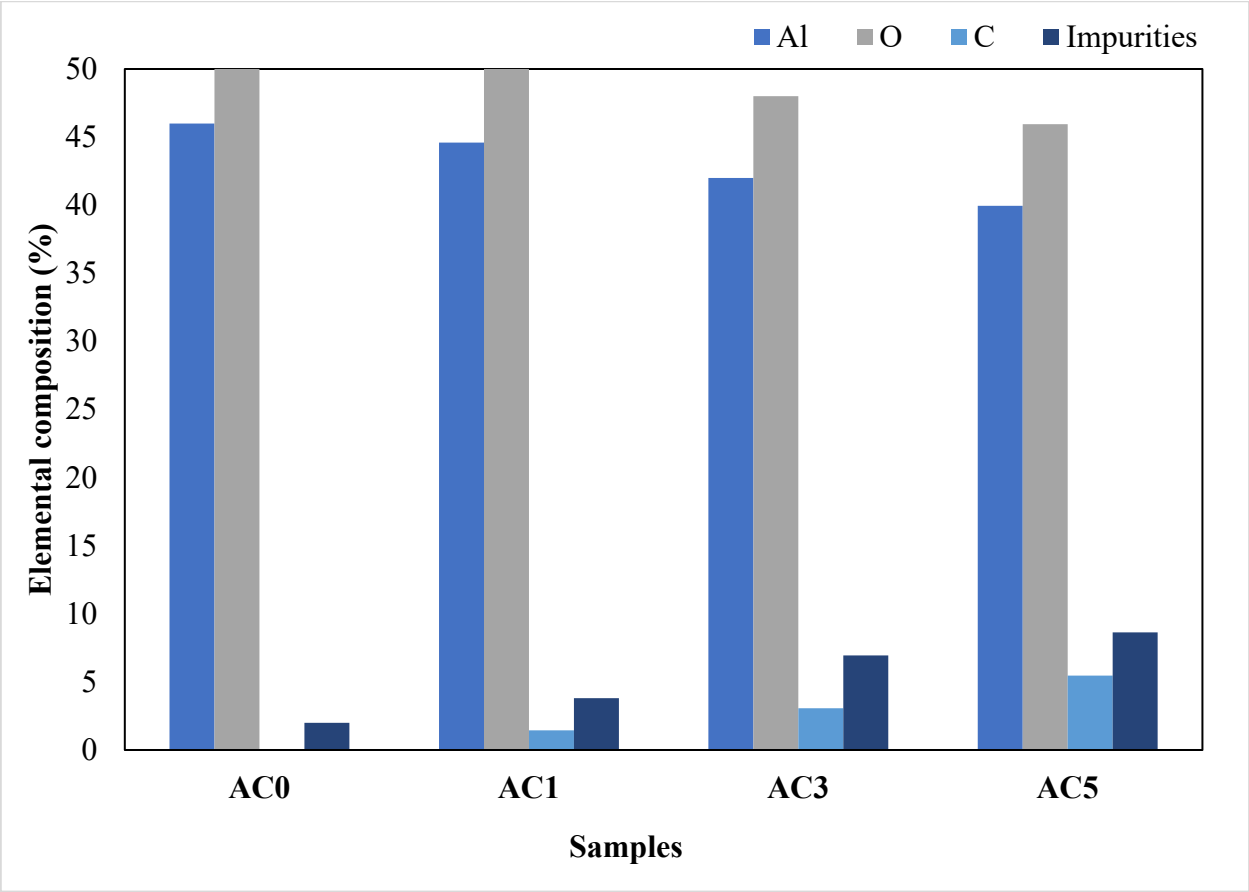

Figure 3. Elemental composition of composites determined through EDS.

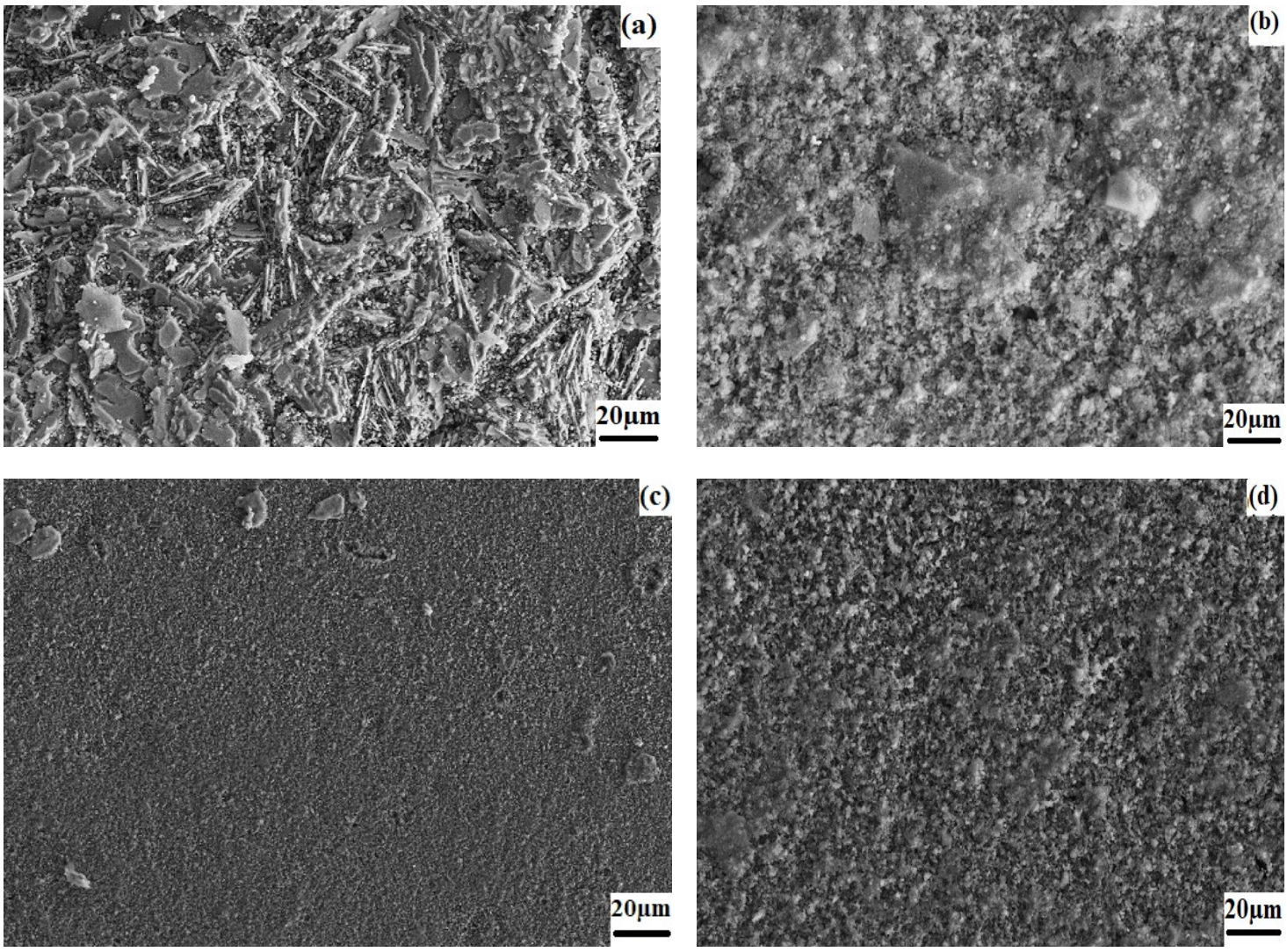

Figure 4. SEM Microstructure of (a) Alumina (AC0) (b) AC1 (c) AC3 and (d) AC5.

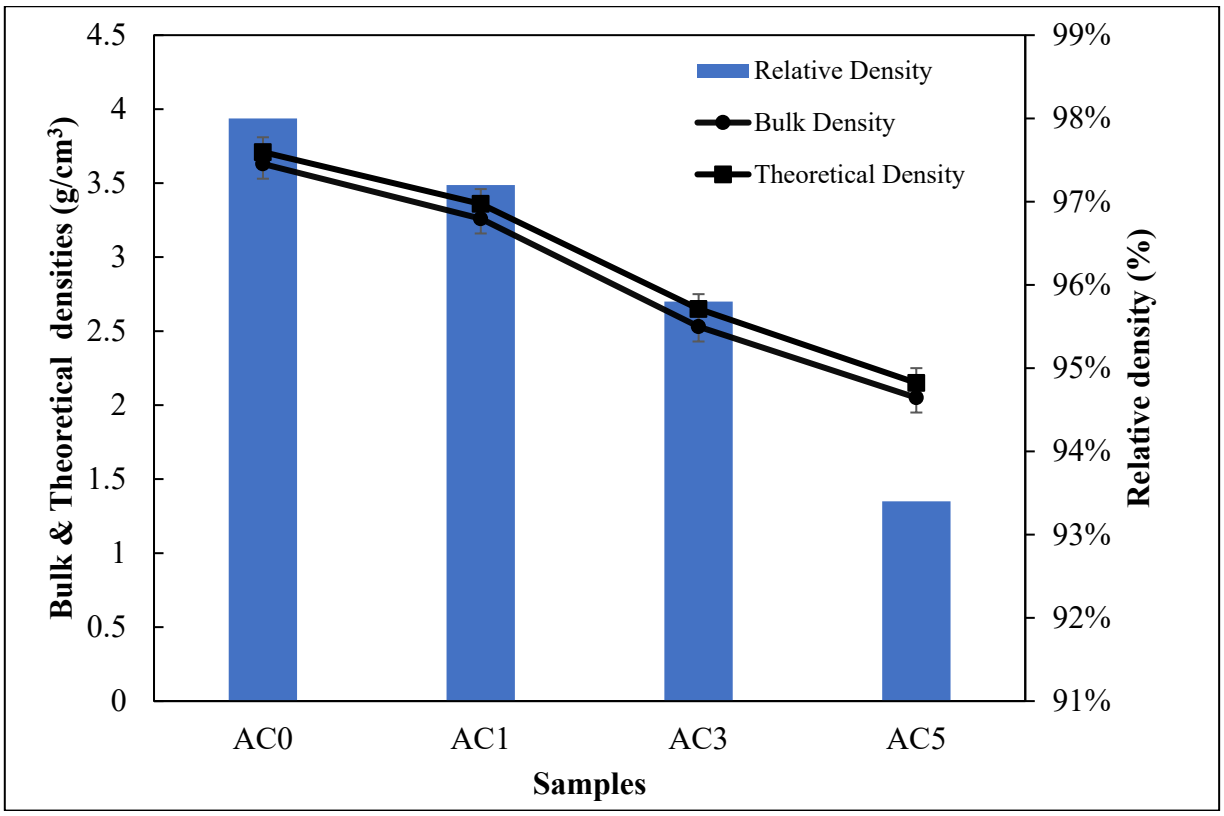

Figure 5. Theoretical, Bulk & Relative Densities of Alumina/MWCNTs nanocomposites.

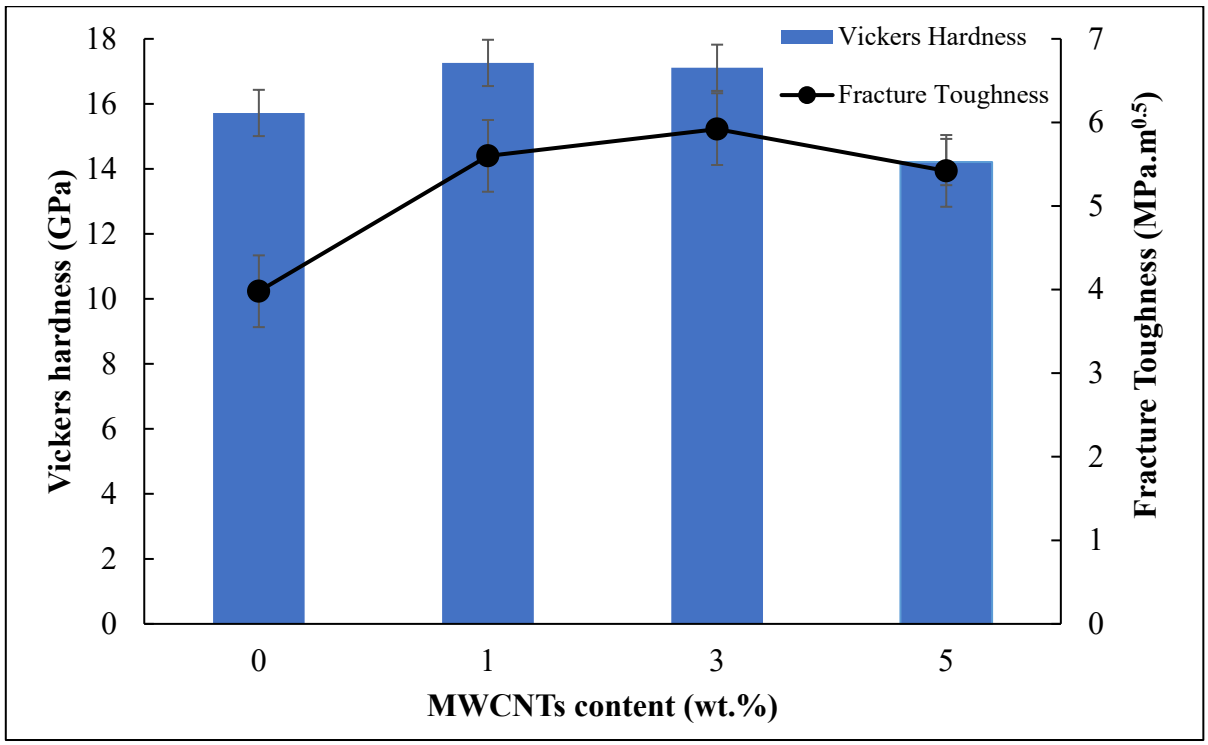

Figure 6. Vickers Hardness and Fracture toughness of nanocomposites plotted as function of MWCNT content.

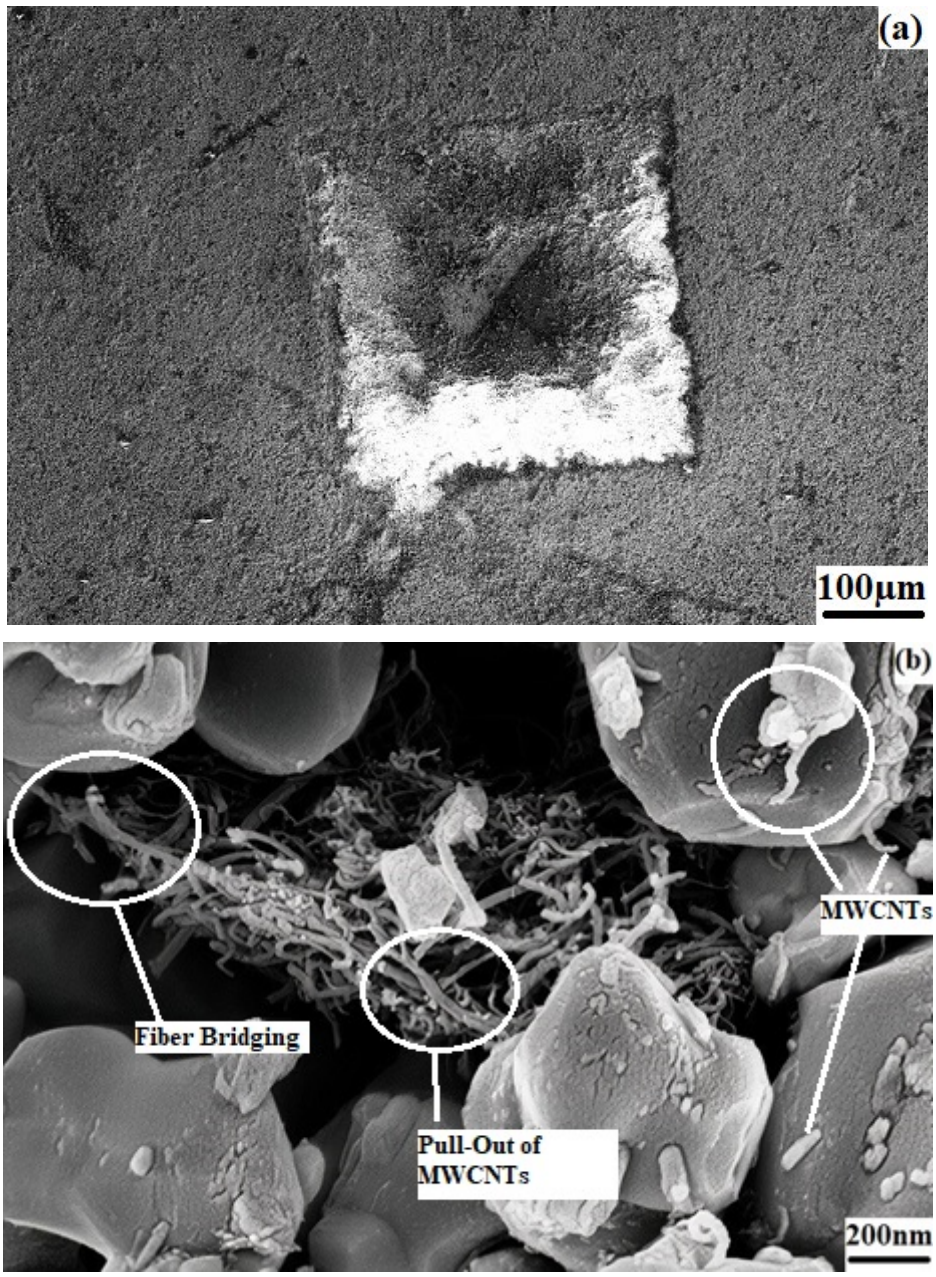

Figure 7. (a) Indentation on AC3 surface (b) MWCNTs bridging and pull-out in AC1.

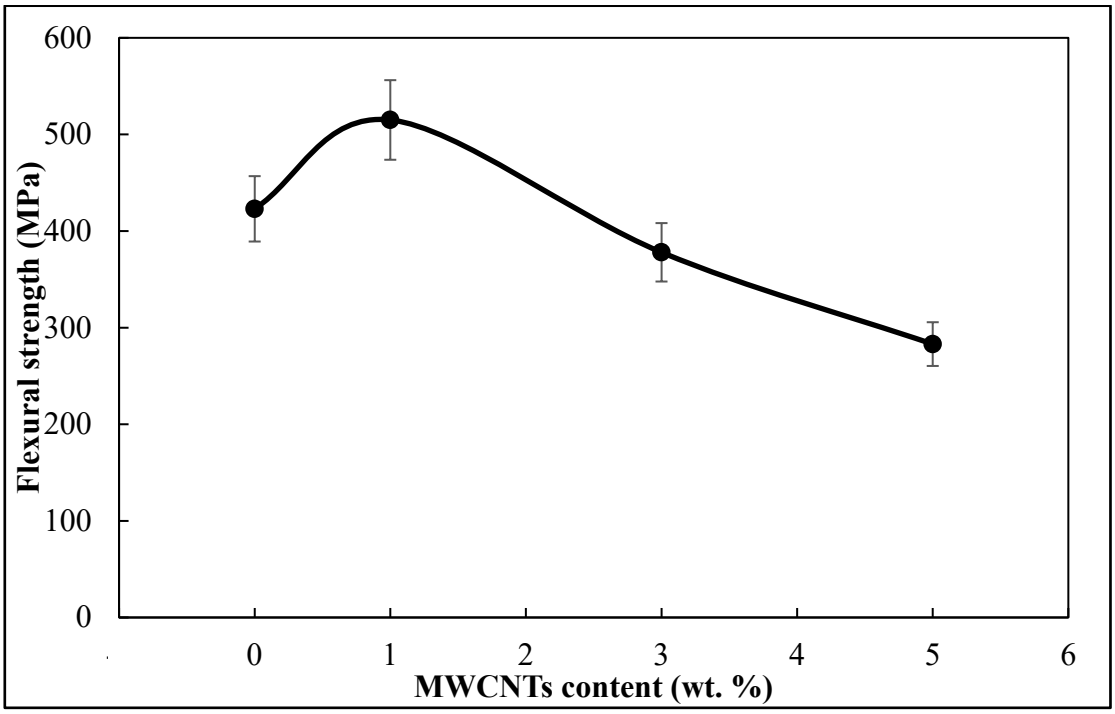

Figure 8. Flexural Strength with respect to MWCNTs content percentage.

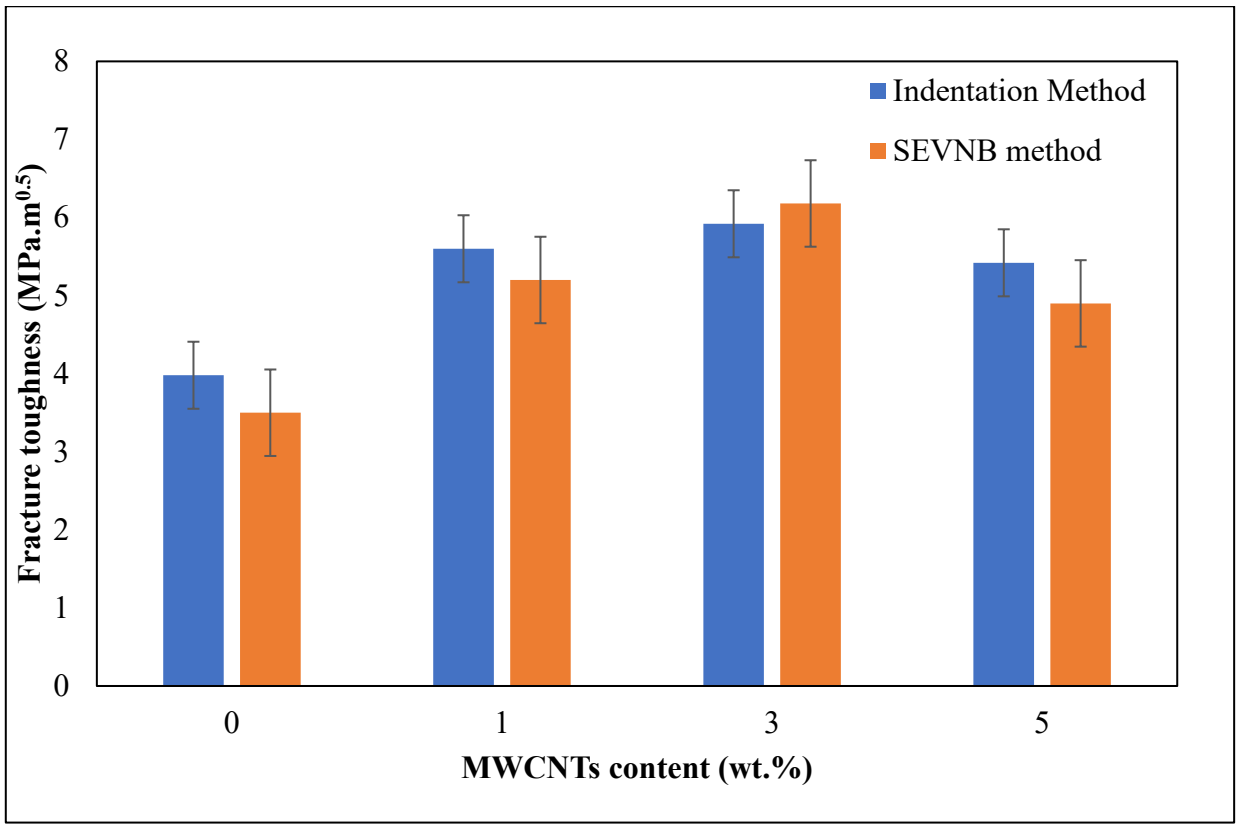

Figure 9. Comparison of SEVNB and indentation method.

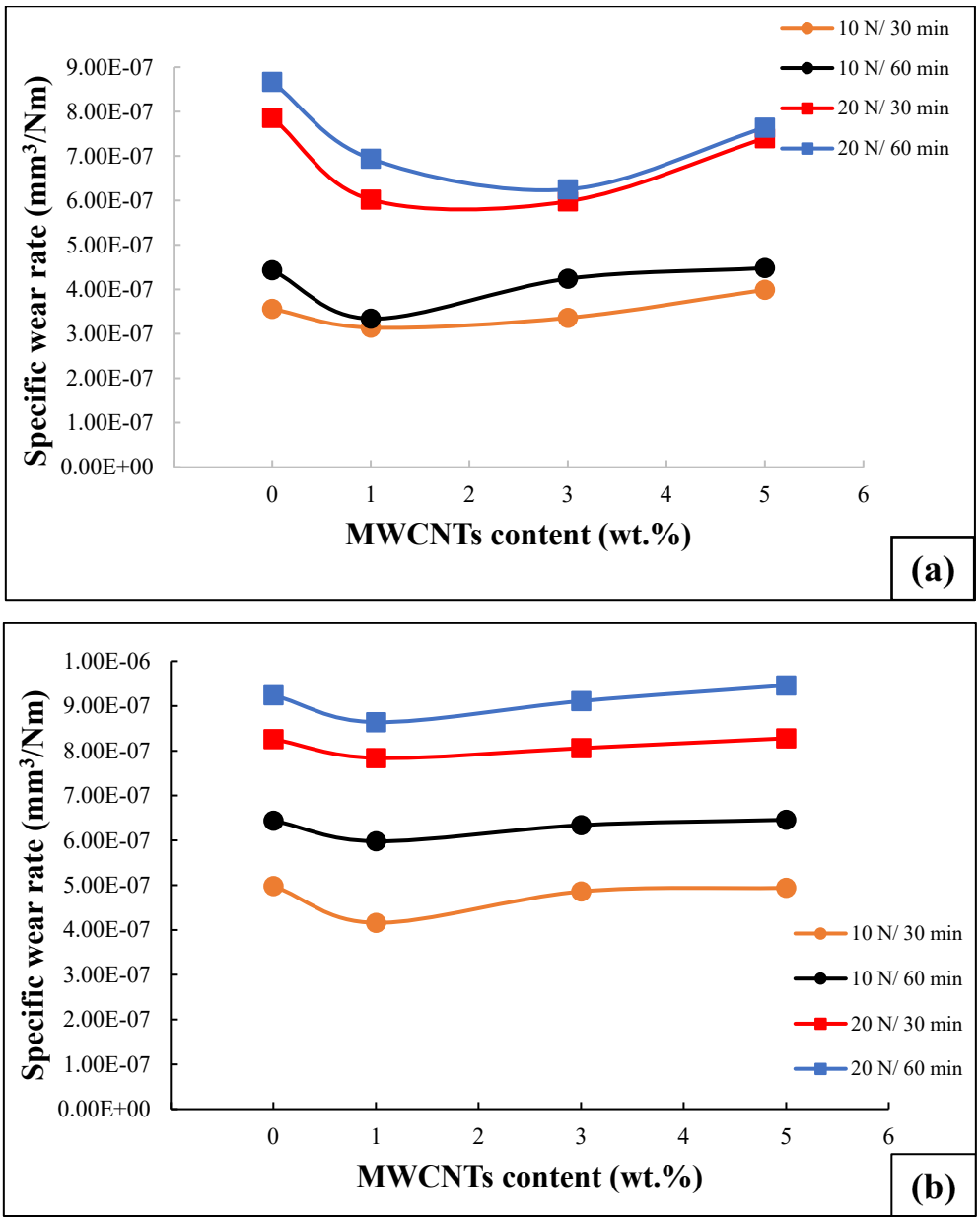

Figure 10. Specific wear rate plotted with respect to MWCNT content (a) 100 m and (b) 400 m.

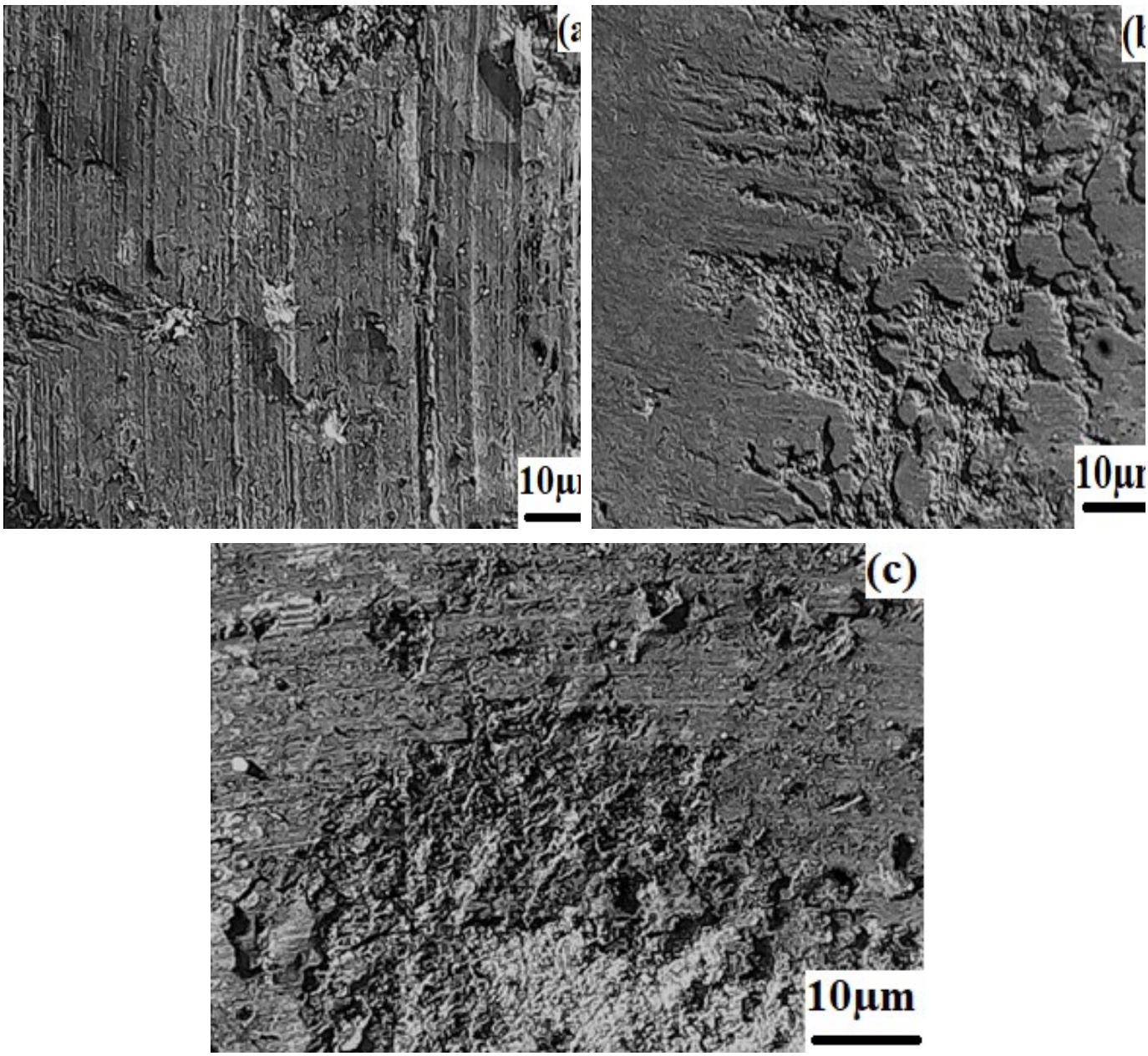

Figure 11. Wear debriefs and cracks in (a) AC1 and (b) AC3 and (c) AC3 composites.

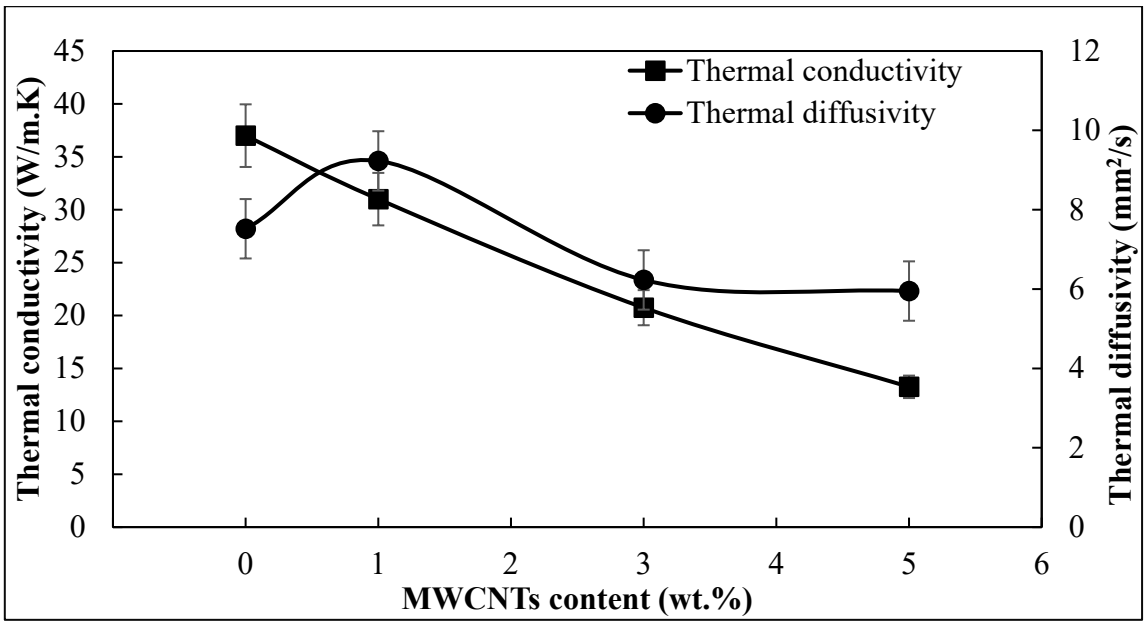

Figure 12. Thermal conductivity and diffusivity of Alumina and its composites as a function of MWCNTs content.